International Journal of Nanomedicine

Dovepress
open access to scientific and medical research

Open Access Full Text Article

ORIGINAL RESEARCH

Biocompatible Assessment of Erythrocyte Membrane-Camouflaged Polymeric PLGA Nanoparticles in Pregnant Mice: Both on Maternal and Fetal/Juvenile Mice

Sailing Chen[1,*], Dongyan Tian[1,*], Xuewei Yang[1,*], Qingqing Yin[1], Li Li[1], Yijing Lin[1], Shuangshuang Liu[1], Huiqian Chen[1], Mingyao Zhang[1], Jiajin Lin[2], Xiaosheng Lu[1], Ping Duan[1], Yijie Chen[1,3,4]

[1]Department of Obstetrics and Gynecology, The Second Affiliated Hospital of Wenzhou Medical University, Wenzhou, People's Republic of China; [2]Department of Blood Transfusion, The Second Affiliated Hospital of Wenzhou Medical University, Wenzhou, People's Republic of China; [3]Cixi Biomedical Research Institute, Wenzhou Medical University, Wenzhou, People's Republic of China; [4]Zhejiang Engineering Research Center for Innovation and Application of Intelligent Radiotherapy Technology, The Second Affiliated Hospital of Wenzhou Medical University, Wenzhou, Zhejiang, People's Republic of China

*These authors contributed equally to this work

Correspondence: Ping Duan; Yijie Chen, Department of Obstetrics and Gynecology, The Second Affiliated Hospital of Wenzhou Medical University, 109 West Xueyuan Road, Wenzhou, 325027, People's Republic of China, Tel +86 577-88002815, Fax +86-577-86689895, Email dppddpp@wmu.edu.cn; chenyijie@wmu.edu.cn

Purpose: Poly(lactic-*co*-glycolic) acid (PLGA) nanoparticles coated with the membrane of red blood cells (RBC-NP) have been applied in various biomedical fields. Despite the well-documented great biocompatibility, the potential toxicity of RBC-NP on maternal mice or their developing fetuses during pregnancy, or juvenile mice post-birth, remains unclear, which warrants a systematic evaluation.

Methods: We fabricate an RBC-NP with approximately 50 nm in diameter (RBC-NP-50). Upon RBC-NP-50, pregnant mice are intravenously injected with this nanoparticle either at a single high dose of 400 mg/kg (1HD) or a low dose of 200 mg/kg for 3 times (3LD). Afterwards, the biocompatible assessments are performed at 48 h after the final injection or 21 d post-birth/partum both on maternal and fetal/juvenile mice.

Results: RBC-NP-50 is capable of accumulating in the placenta and then passing through the blood-fetal barrier (BFB) into the fetus. On 48 h after RBC-NP-50 exposure, no significant dose-dependent toxicity is observed in maternal mice including blood biochemistry, inflammatory factors, progesterone level, histological analysis, etc, whereas fetal brains reveal remarkable differentially expressed genes analyzed by transcriptome sequencing. On 21 d post-birth, those genes' expression in juvenile mice is alleviated, along with negligible differences in behavioral evaluations including surface righting test, negative geotaxis test, cliff avoidance test, and olfactory orientation test.

Conclusion: These results indicate that RBC-NP is considered to be generally safe and biocompatible both for maternal mice and fetus during pregnancy, and for the subsequent juvenile mice post-birth, although future studies will need to examine higher dosage or longer-term measurements.

Keywords: erythrocyte membrane, pregnancy, fetus, biocompatibility, RNA sequencing

Introduction

Red blood cell (RBC) membrane-coated PLGA nanoparticle (RBC-NP) is fabricated through a top-down approach that translocates the intact membrane of RBC onto the PLGA core.[1–3] Following this strategy, RBC-NP faithfully inherits the protein repertoire from the parents' RBCs without compromising their functionalities, which has been broadly used for wide applications.[4–6]

Received: 8 August 2022
Accepted: 15 November 2022
Published: 1 December 2022

More recently, RBC-NP represents a broad-spectrum detoxification nanodecoy to absorb "toxins" that target specific receptors or lipid structures of intended RBCs. For example, RBC-NP exhibits the ability to capture autoantibodies regarding antibody-antigen specificity,[7] to detain bacterial exotoxins regardless of their structural identities[8–10] and to sequester chemical toxicants via a stoichiometric binding pattern.[11] It is noteworthy that the bacterial exotoxins arrested by RBC-NP, denoted "nanotoxoid", could translate the exotoxins into a safe and effective vaccine for immune processing.[12,13] Additionally, RBC-NP loaded with anticancer drugs could work as a new drug delivery system due mainly to the protein makeup displayed on the RBC surface that contributes to long circulation, leads to enhanced cancer suppression efficacy.[14,15] Further, a more impressive anticancer outcome of RBC-NP could be achieved by additional surface modification with a specific cancer-targeting ligand.[16,17] Also, an improved antibacterial effect could be as well as obtained after incorporating bactericidal drugs into RBC-NP.[18] Besides these, RBC-NP's function could be further extended by fusing with other cell membranes[19–21] or by loading other functionalized modules including perfluorocarbon for oxygen delivery.[22] More significantly, RBC-NP combines the advantages of natural RBC membrane and FDA-approved materials PLGA, is considered a great biocompatible biomimetic platform.[23,24] Thus far, the given efforts have preeminently focused on the extensive applications of RBC-NP, yet a comprehensive estimation of the biosafety of RBC-NP itself is still missing, particularly in pregnant mice referring to maternal systemic toxicity and developmental interference to their fetuses or the subsequent juvenile mice post-birth. Therefore, a systematic biosafety evaluation of RBC-NP in both pregnant mice and their offspring with more thorough studies is urgently needed, not only looking at the tissue structure and biochemical markers but also investigating the changes at transcriptional levels.

Herein, we reported an ultra-small RBC-NP with a diameter of nearly 50 nm (RBC-NP-50) that was capable of crossing the placenta effectively and readily entering the fetus, which provided a suitable size required for investigating the dose-dependent toxicity of RBC-NP on both maternal and fetal/juvenile mice. Dosed pregnant mice with RBC-NP-50 following the different dosing regimens, including a single high dose of 400 mg/kg (1HD) and an thrice successive low dose of 200 mg/kg (3LD), the biocompatible assessments were performed at 48 h after the final injection or 21 d post-birth/partum both on maternal and fetal/juvenile mice (Figure 1).

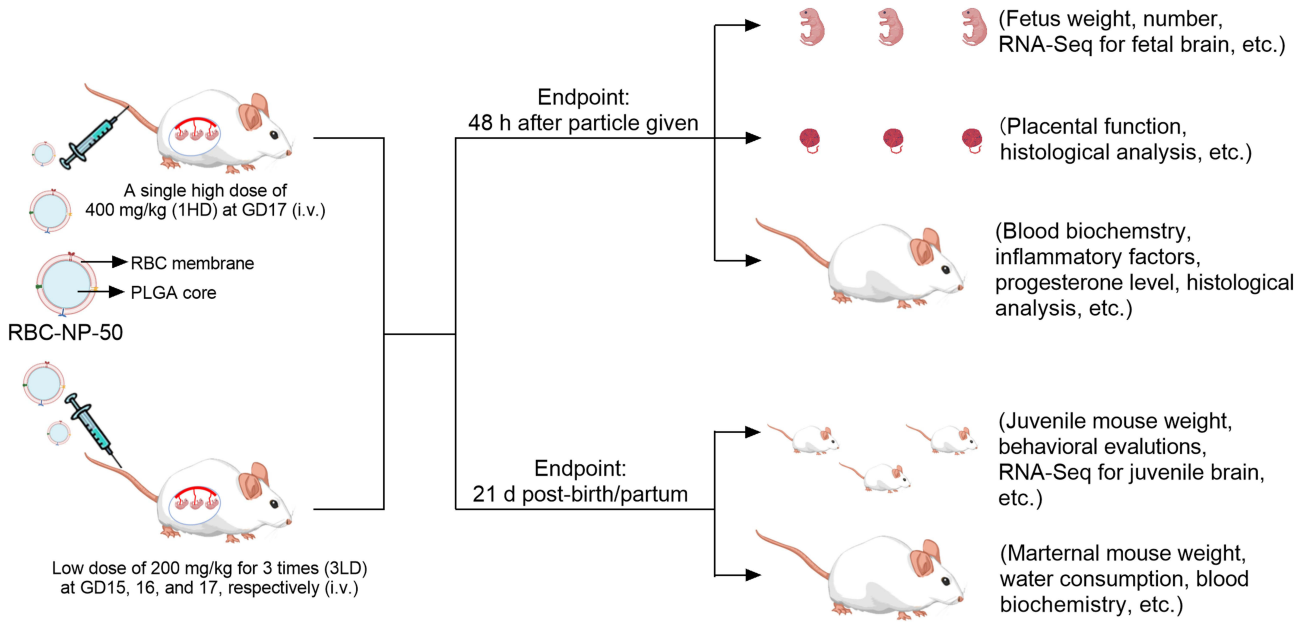

Figure 1 Schematic workflow. For dosing regimens design, pregnant ICR mice at GD17 were administrated with RBC-NP-50 at 400 mg/kg (denoted 1HD) by i.v.; or pregnant mice were repeatedly successive dosed with 200 mg/kg of RBC-NP-50 by i.v at GD15, 16, and 17 for three times (denoted 3LD). For testing regimens, at 48 h following the final injection of either 1HD or 3LD of RBC-NP-50, the related parameters from maternal mice and fetuses were tested; or the related measurements upon maternal and juvenile mice were monitored/tested throughout the experiment until 21 d post-partum/birth.

Materials and Methods

RBC Membrane Derivation

Whole blood was collected from ICR mice through submandibular puncture with an EDTA-coated tube (BD Microtainer). The obtained whole blood was subjected to a centrifugation of 800 rcf for 5 min. After the serum and buffy coat removal, the RBCs were treated by a hypotonic method. Briefly, the palleted RBCs were resuspended in sixfold volume of water and incubated for 10 min at room temperature (RT). Afterwards, the RBCs suspension was adjusted to 1 × PBS with 20 × PBS, followed by centrifuging at 12,000 rcf for 10 min. The above process was repeated until the resultant supernatant was undetectable hemoglobin. By discarding the supernatant, the RBC membrane precipitation was dispersed in water and the membrane protein was quantified using bicinchoninic acid (BCA) assay (Thermo Fisher, Waltham, MA, USA) according to the vendor's instructions. Before use, the RBC membrane was stored in −80°C.

Preparation and Characterization of Different-Sized RBC-NP

Carboxyl group-terminated 50:50 poly(lactic-*co*-glycolic(acid (PLGA) was purchased from Lactel Absorbable Polymers (Pelham). PLGA nanoparticles with diameter of 30 and 150 nm were prepared by the nanoprecipitation method. To make 30 nm of PLGA nanoparticle, PLGA (dissolved in acetone) at 7 mg/mL in 10 mL was quickly added into 30 mL pre-cold water containing 10 mM of Tris-HCl. The organic solvent was evaporated using a vacuum chamber. To prepare 150 nm of PLGA nanoparticle, 2 mL of water was injected into 1 mL of PLGA acetone solution (20 mg/mL). The mixture was subjected to a vacuum chamber for acetone removal. PLGA of 450 and 1000 nm in diameter were synthesized by the single emulsion method. To make 450 nm of PLGA nanoparticle, 0.5 mL of PLGA dissolved in dichloromethane (DCM) at 60 mg/mL was added into 5 mL of 2.5% PVA (w/v) solution, followed by a probe ultrasonication treatment (60 W, 2 s on/ 2 s off, for 3 min) (150E Sonic Dismembrator, Thermo Fisher). After that, the DCM was evaporated through a vacuum chamber. To fabricate 1000 nm of PLGA particle, 1 mL of 60 mg/mL PLGA (dissolved in DCM) was mixed with 10 mL of 2.5% PVA (w/v), followed by treated with a homogenizer (WIGGENS, D-130) at 15,000 rpm for 5 min. Likewise, the organic solvent was removed by evaporation.

Upon the different sizes of PLGA particles, the various RBC-NP particles were fabricated by mixing PLGA particles with RBC membrane (the weight ratios of PLGA to membrane protein were calculated in Supplementary Table 1), followed by sonicating with a bath ultrasonicator (FB15051, Fisherbrand, Germany) at 120 W for 3 min. Diameters and surficial charges in four sizes of RBC-NP were characterized by dynamic laser scattering (DLS), and their colloidal stability curves dispersed in PBS were also monitored over 7 days. The resultant various sizes of RBC-NP were denoted as RBC-NP-50, RBC-NP-180, RBC-NP-400, and RBC-NP-1000. To fluorescently label PLGA core, 1,1'-dioctadecyl -3,3,3',3'-tetramethylindodicarbocyanine 4-chlorobenzenesulfonate salt (DiD) dissolved in acetone was premixed with PLGA at a 2 wt% ratio prior to the synthesis of different PLGA particles. Afterwards, DiD-labeled RBC-NP was fabricated by the process samilar to that for RBC-NP.

At the determined size of RBC-NP-50, the morphology of this nanoparticle was visualized by transmission electron microscopy (TEM). Briefly, RBC-NP-50 at 0.5 mg/mL was dropped onto holey carbon-coated Cu grids, followed by negatively staining with 1% uranyl acetate. After drying, images of RBC-NP-50 were photographed using a TEM device (JEM-2100F, JEOL, Japan). The protein compositions of RBC-NP-50 were analyzed by sodium dodecyl sulfate polyacrylamide gel electrophoresis (SDS-PAGE) method. Briefly, RBC-NP-50 at 1 mg/mL was mixed with 5 × lithium dodecyl sulfate loading buffer, followed by heating at 90 °C for 10 min. After transferring to a 12-well Blot 4–12% SDS-PAGE gel, samples were run at 120 V for 30 min. Following the electrophoresis, the gel was stained with Coomassie Blue. Furthermore, the specific proteins in RBC-NP-50, including CD47 and CD36 were characterized by Western blot. After electrophoresis, all proteins in the gel were translocated onto PVDF membrane (Millipore, Bedford, USA) at 300 mA for 90 min. Then, samples were blocked with 5 × Protein Free Rapid Blocking Buffer (Epizyme, China) for 10 min and incubated with CD47 (1:200 dilution, Abcam) and CD36 (1:200 dilution, Abcam, Shanghai, China) primary antibodies overnight at 4 °C. After removal of free antibodies, the PVDF membrane was washed with PBST (containing 0.1% Tween-20) for three times, followed by the addition of horseradish peroxidase (HRP)-conjugated secondary antibody (Invitrogen, Beijing, China) for another 1 h. After washing with PBST (containing 0.1% Tween-20), the blot

signals in membrane were visualized by an enhanced chemiluminescence detection kit (EpiZyme, Shanghai, China) and were photographed by a ChemiDoc CRS imaging system (Bio-Rad, USA).

Animal Care

All the animal procedures complied with the guidelines of the Laboratory Animal Ethics Committee of Wenzhou Medical University & Laboratory Animal Centre of Wenzhou Medical University in Wenzhou, China (wydw2022-0536). ICR mice were housed in sterile cages with a consistent temperature range of 24–26 °C under a 12 h light/dark cycle. All mice had free access to food and water.

Screening an Optimal Size of RBC-NP to Pass Through Placenta in Pregnant Mice

Pregnant ICR mice at gestation day 16 (GD16) were intravenously injected with four sizes of DiD-labeled RBC-NP, respectively, including RBC-NP-50, RBC-NP-180, RBC-NP-400, and RBC-NP-1000. The dosage of four sized RBC-NP was at an equivalent PLGA dosage of 50 mg/kg. At 24 h after particle injection, the pregnant mice were euthanized and the placentas and fetuses were harvested and then imaged and analyzed by IVIS Lumina XRMS Series III (PerkinElmer, USA). To investigate the time-dependent distribution of RBC-NP-50 to both placenta and fetus, DiD-labeled RBC-NP-50 at 50 mg/kg (referred to as PLGA dosage) was injected by i.v. at GD14, 15, 16, or 17. At 24 h post each injection, the placentas and fetuses from pregnant mice were collected and then photographed and analyzed by IVIS Lumina XRMS Series III (PerkinElmer, USA). Mice treated with vehicle solution (8% sucrose, w/v) were used as controls.

Biocompatibility of RBC-NP-50 in vitro

BeWo and HUVEC cells were purchased from Procell (Wuhan, China). BeWo and HUVEC cells were cultured in Ham's F-12K (Kaighn's) and 1640 medium, respectively, and all were supplemented with 10% fetal bovine serum and 1% penicillin–streptomycin. Cells were incubated in a 5% CO_2 humidified incubator at 37 °C. To test the biocompatibility of RBC-NP-50 on these two cells, various concentrations (including 7.8, 15.6, 30.3, 62.5, 125, 250, 500, and 1000 μg/mL) of RBC-NP-50 were co-incubated with cells that pre-cultured in 96-well plates with 80% confluence for 24 h. Afterwards, the cell viability was tested with CCK-8 assay following the vendor's instructions.

Biodistribution Study of RBC-NP-50 in Pregnant Mice

RBC-NP-50 labeled with DiD at 50 mg/kg were injected by i.v. into pregnant ICR mice at GD15. At predetermined time points, including 24 h, 48 h, and 72 h after particle administration, major organs (including the liver, kidneys, spleen, brain, lungs, and heart), whole blood, placentas, and fetuses were collected and weighed. Whole blood at 30 μL was added to 70 μL of water, and the mixture was subjected to test the fluorescence with a plate reader at an excitation/emission of 630/670 nm. Meanwhile, the fluorescence intensity in tissues was measured by adding PBS (1 g tissue added into 1 mL PBS) and then treated with homogenization, followed by analyzing the fluorescent signal at an excitation/emission of 630/670 nm using a plate reader. Mice treated with PBS only were used as negative controls.

Dosing and Testing Regimens in vivo

For dose choice, we firstly concentrated the RBC-NP-50 as high as possible, and then we found the highest injectable concentration was nearly of 50 mg/mL (cell membrane protein) otherwise would go to gel status. On the other hand, the acceptable injection volume regarding mouse ethics is less than 500 μL; thus we selected 400 μL per mouse. The average weight of pregnant mouse at later stage of gestation is about 50 g, and we thus figured out a single high dose (denoted 1HD) of RBC-NP-50 at 400 mg/kg. Parallelly, a thrice successive low dose (denoted 3LD) of RBC-NP-50 at 200 mg/kg was chosen as another experimental group. Each injection of 3LD was half compared to 1HD, but 1.5-fold higher than 1HD in total. For dosing frequency, we first demonstrated that RBC-NP-50 could accumulate in placenta and fetus and reach plateau around GD17 (Figure 2E and F). Refering to an average parturition time point of mouse is about GD21, we thus picked the GD17 as the final injection time both for 1HD and 3LD. Taken together, pregnant mice at GD17 were administrated with RBC-NP-50 at 400 mg/kg by i.v.; or pregnant mice were repeatedly successive dosed with 200 mg/kg

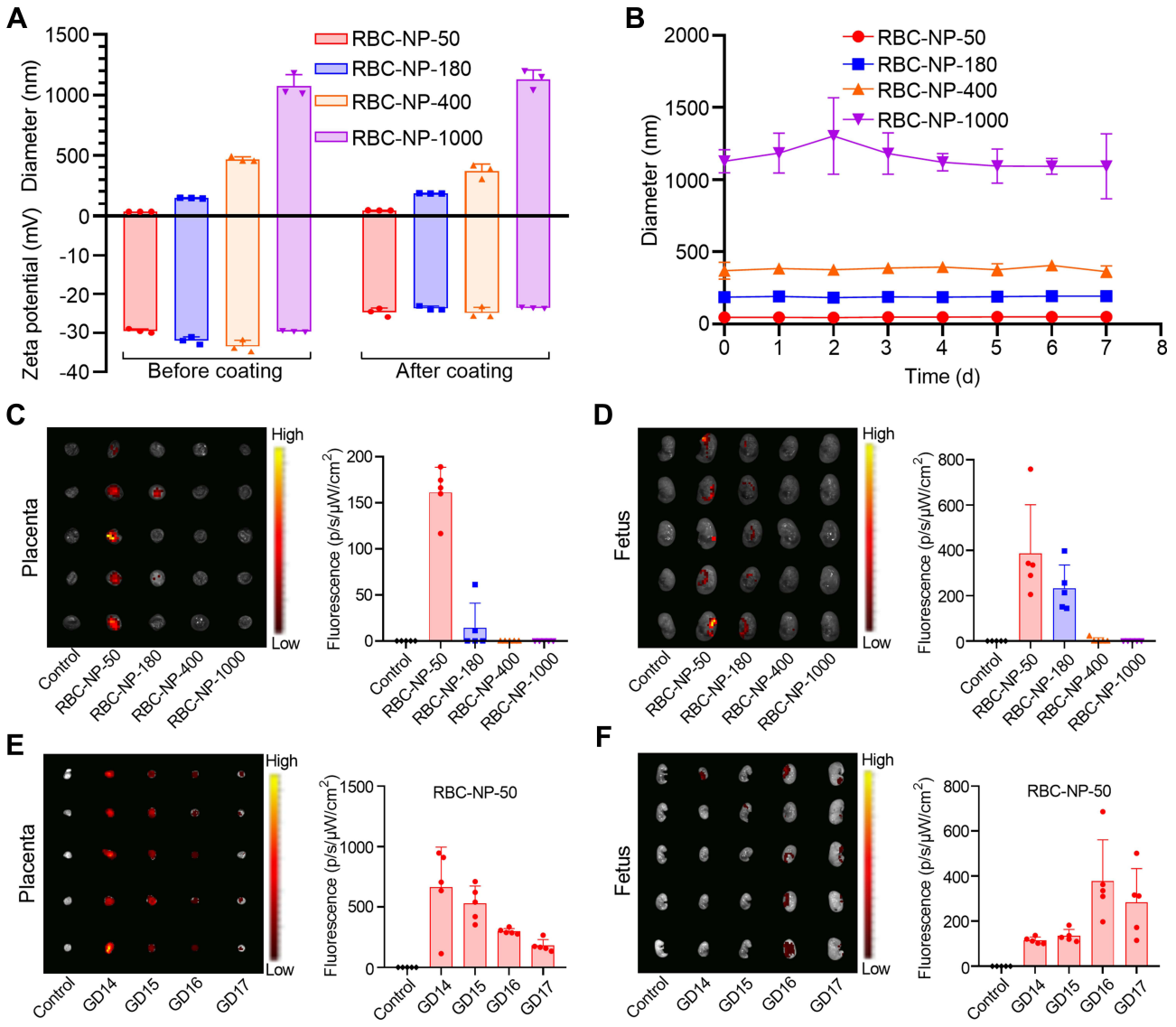

Figure 2 Biodistribution of RBC-NP at different sizes in pregnant mice. (**A**) Hydrodynamic size (diameter) and zeta potential (mV) of different nanoparticles before and after RBC membrane coating. n = 3, mean ± SD. (**B**) Colloidal stability of different RBC-NP particles in PBS over 7 days. n = 3, mean ± SD. Fluorescent images and statistical analysis showing different accumulations in placentas (**C**) and fetuses (**D**) of pregnant mice after being injected with various sizes of DiD-labelled RBC-NP particles by i.v., including RBC-NP-50, RBC-NP-180, RBC-NP-400, and RBC-NP-1000. n = 5, mean ± SD. Fluorescent images and statistical analysis showing different accumulations in placentas (**E**) and fetuses (**F**) of pregnant mice after being injected with DiD-labelled RBC-NP-50 at different gestation day (GD), including GD14, 15, 16, and 17. n = 5, mean ± SD.

of RBC-NP-50 by i.v. at GD15, 16, and 17 for three times. At each dosing regimen, mice treated with an identical volume of 8% (w/v) sucrose were used as controls.

For testing regimens, at 48 h (GD19) following the final injection of either 1HD or 3LD of RBC-NP-50, pregnant mice in all groups were euthanized and the related parameters both from maternal mice and their fetuses were tested; or the related measurements upon maternal and juvenile mice were monitored/tested throughout the duration until 21 d post-partum/birth.

Biocompatible Assessment of RBC-NP-50 on Maternal Mice and Fetuses in Short Term (48 h After Final Injection)

Pregnant ICR mice were intravenously injected with 1HD or 3LD of RBC-NP-50 as described in "Dosing and testing regimens in vivo" section, followed by collecting major organs (including heart, liver, spleen, lungs, and kidneys), placentas,

fetuses, and blood at 48 h after final injection. In first, cytochrome P450 family 11 subfamily A member 1 (CYP11A1) expression in the placenta was determined by Western blot. Briefly, proteins within placental tissues were freshly extracted with a RIPA lysis buffer (Millipore, Billerica, MA) and quantified by BCA assay. All samples were then mixed with 5 × lithium dodecyl sulfate sample loading buffer and heated at 95 °C for 5 min. Following heating, samples were transferred to SDS-PAGE gel (4–12%) and ran at 150 V for 30 min. Afterwards, the resultant gel was placed onto a PVDF membrane and subjected to 300 mA for 90 min. After blocking with 5 × Protein Free Rapid Blocking Buffer for 10 min, the membrane was immunostained with CYP11A1 (1:200 dilution, Bioss, Beijing, China), GAPDH (1:200 dilution, ABclonal, Wuhan, China), and 3β-hydroxysteroid dehydrogenase (3β-HSD) (1:200 dilution, ABclonal, Wuhan, China) primary antibodies for 2 h. After incubation, the membrane was washed with PBS containing 0.05% Tween 20 for three times, followed by incubating with HRP-conjugated secondary antibody (Biolegend, California, USA) for another 1 h. After the addition of ECL substrate (Meilunbio, Dalian, China), blot signals were visualized and analyzed by an imaging system (ChemiDoc TM XRS +, Bio-Rad). Meanwhile, the angiogenesis-related protein, CD34, was tested in the placenta. Briefly, placentas were fixed with 4.0% paraformaldehyde, and dehydrated with an ethanol gradient. The samples were then embedded into paraffin and cut into sections. After blocking with 10% bovine serum albumin (BSA, Solarbio, Beijing, China), the sections were incubated with a CD34 primary antibody (1:200 dilution, Zen-Bioscience, Chengdu, China) at 4 °C overnight. After removal of free antibodies, the membrane was washed thrice with PBS, and the sections were incubated with a HRP-conjugated secondary antibody for 1 h at RT. After incubation, the slides were treated with a 3,3'-diaminobenzidine (DAB) chromogen kit, and images were taken by a light microscope. In parallel, the progesterone and three key inflammatory factors including interleukin 6 (IL-6), tumor necrosis factor α (TNF-α), and monocyte chemoattractant protein-1 (MCP-1) in blood were measured by enzyme-linked immunosorbent assay (ELISA). Whole blood at 600 μL was collected through the submandibular puncture and allowed to coagulate. Serum samples were separated by centrifuging at 2000 rcf for 10 min. Then, all samples were subjected to the respective ELISA kits (Elabscience, Wuhan, China) according to the manufacturer's instructions. The absorbance of samples at 450 nm was measured with a plate reader. Furthermore, hematological and biochemical analyses were performed to evaluate the biocompatibility of RBC-NP-50 in maternal mice. Upon serum collection, biochemistry parameters were measured by Beckman Coulter (AU480). Meanwhile, 50 μL of whole blood was collected into anti-coagulation coated tubes and then subjected to detect blood routine parameters by a hematology analyzer (Biote, HL-2400). For histological estimation, the harvested major organs and placentas were stained with HE kit following the manufacturer's instructions and photographed by light microscopy.

On the other hand, fetuses were counted and weighed in all groups. Moreover, to investigate the transcriptomic changes in the fetal brains, high-throughput mRNA sequencing was utilized. Upon fetal brain collection, total RNA was extracted with TRIzol reagent (Invitrogen, Beijing, China) according to the manufacturer's protocol. RNA purity and quantification were determined using NanoDrop 2000 spectrophotometer (Thermo Scientific, Beijing, China). RNA integrity was assessed by Agilent 2100 Bioanalyzer (Agilent Technologies). Then, the libraries were constructed using a TruSeq Stranded mRNA LT Sample Prep Kit (Illumina) according to the manufacturer's instructions. The transcriptome sequencing and analysis were carried out by OE Biotech Co. Ltd. (Shanghai, China). P value <0.05 and foldchange >2 or foldchange <0.5 was set as the threshold for a significant differential expression. Hierarchical cluster analysis of Differentially Expressed Genes (DEGs) was performed to demonstrate the expression patterns of genes in different samples. To evaluate the biological functions, the significantly altered mRNAs were analyzed by performing a Gene Ontology (GO) analysis. The Kyoto Encyclopedia of Genes and Genomes (KEGG) pathway enrichment analyses of DEGs were performed using R language based on the hypergeometric distribution. After the reads were assembled by StringTie, gene structure extension and novel transcripts identification were performed by comparing the reference genome and the known annotated genes using Cuffcompare software.

Biocompatible Assessment of RBC-NP-50 on Maternal and Juvenile Mice in Long Term (21 d Post-Partum/Birth)

Pregnant ICR mice were intravenously dosed with 1HD or 3LD of RBC-NP-50 as described in "Dosing and testing regimens in vivo" section, followed by housing until delivery. After giving birth, the maternal and newborn mice were

fed to 21 d post-partum/birth. From GD13 to 19 d post-partum, body weight and water consumption of maternal mice were monitored. At 21 d post-partum, maternal mice were euthanized and the inflammatory factors (including IL-6, TNF-α, and MCP-1) in blood were tested using ELISA kits. Meanwhile, hematological and biochemical analyses were carried out. Briefly, 600 μL of whole blood was collected through the submandibular puncture and allowed to coagulate. Biochemical parameters in serum were measured by Beckman Coulter. Meanwhile, 50 μL of whole blood was collected into anti-coagulation-coated tubes and then subjected to detect blood routine parameters by a hematology analyzer.

On the other hand, the number of newborn mice after maternal delivery was enumerated. Afterwards, body weight gaining of all juvenile mice was recorded over 21 days. Throughout the duration of 21 d post-birth, the behavioral evaluations of juvenile mice were performed, including surface righting test, negative geotaxis test, cliff avoidance test, and olfactory orientation test. In surface righting test, juvenile mice at 5 d post-birth were placed on their backs on a pad, and then counted the time they needed to right themselves. This was scored based on the successful righting time: within 1 sec, 2 scores; between 1 and 2 sec, 1 score; more than 2 sec, 0 score. In the negative geotaxis test, juvenile mice at 7 d post-birth were placed in a head-down position on a 45° inclined plane covered with sandpaper (fine grade), and then counted the time they needed to face up. This was scored based on the successful facing up time: within 30 sec, 2 scores; between 30 sec and 60 sec, 1 score; no response within 60 sec, 0 score. In the cliff avoidance test, juvenile mice at 7 d post-birth were placed with the digits only of their forepaws and their snout positioned over a flat elevated edge. This was scored based on the successful avoidance time: avoiding with turn, 2 scores; walking backwards within 20 sec, 1 score; no response within 20 sec, 0 score. In olfactory orientation test, an apparatus consisted of two compartments, in which one was covered with used wood flakes and the other was covered with fresh wood flakes. Upon the preparation, juvenile mice at 14 d post-birth were placed in the arm between the two compartments, and the olfactory orientation scored. Entering into the compartment with used wood flakes directly, 2 scores; entering into the compartment with used wood flakes after have stayed the compartment with fresh wood flakes, 1 score; no any response within 90 sec, 0 score.

Furthermore, transcriptomic changes in brains of juvenile mice at 21 d post-birth were likewise performed by high-throughput mRNA sequencing, followed by analysis using DEGs, GO, and KEGG according to the mentioned method in the section "Biocompatible assessment of RBC-NP-50 on maternal mice and fetuses in short term (48 h after final injection)".

Statistical Analysis

The data are presented as the mean ± SD and are representative of at least three independent experiments. Statistical significance was determined by a two-tailed unpaired Student's *t*-test. Comparisons between groups were analyzed with one-way analysis of variance (ANOVA). *$p<0.1$, **$p<0.01$, ***$p<0.001$, and ****$p<0.0001$.

Results and Discussions

Determining a Suitable Size of RBC-NP Required for the Biosafe Assessment in Pregnant ICR Mice

In order to seek a proper size of RBC-NP that could cross the placenta of pregnant mice and enter the fetus, we firstly prepared various sizes of poly(lactic-*co*-glycolic) acid (PLGA) core including approximately 30 nm, 150 nm, 400 nm, and 1000 nm measured by DLS (Figure 2A) and visualized by TEM (Supplementary Figure 1A). All four sizes of PLGA particles were about 20 nm increment after coating with RBC membrane respectively via the electrostatic repulsion effect under bath sonication,[27] along with surface charges all elevated (Figure 2A and Supplementary Figure 1B), indicating the successful cloaking of membranes onto PLGA cores. The resulting different sizes of RBC-NP were denoted as RBC-NP -50, RBC-NP-180, RBC-NP-400, and RBC-NP-1000. After dispersing these four sizes of RBC-NP particles in PBS, little change in size was detected over 7 days, indicating the RBC membrane coating was effective at conferring great colloidal stability (Figure 2B). We next aimed to test which size of RBC-NP could preferentially pass through the placenta of pregnant mice and enrich in the fetus. At 24 h after intravenously injecting the four sizes of DiD-labelled RBC-NP at an equivalent PLGA dose of 50 mg/kg with comparable fluorescence intensity (Supplementary Figure 2) into pregnant mice at GD16, the placentas and fetuses were collected for fluorescence analysis. It was shown that the pregnant mice treated

with RBC-NP-50 exhibited the highest fluorescence intensity in the placenta, vs fewer in RBC-NP-180 group and undetectable in both RBC-NP-400 and RBC-NP-1000 groups (Figure 2C). This enhanced enrichment of RBC-NP-50 in placentas as well as resulted in elevated fluorescence level in the corresponding fetuses (Figure 2D). Also, accumulation of RBC-NP-50 in placenta showed a gestation day-dependent decrement manner while the gradually increased in the corresponding fetuses, in agreement with the previous studies claiming that the formation and maturation of blood–fetal barrier (BFB) allows the nanoparticles to translocate easily (Figure 2E and F).[19] Interestingly, the RBC-NP-50 mainly localized to the fetal brains due to the loose blood-brain barrier (BBB) in the developing fetus during pregnancy, and this phenomenon reasoned that further analysis of the development of fetal brains is highly desirable when they are exposed to RBC-NP-50 directly.

Characterization of RBC-NP-50

After having determined RBC-NP with a diameter of nearly 50 nm (RBC-NP-50) as a suitable size for subsequent studies, its physicochemical and biological properties were characterized. Morphology of RBC-NP-50 was visualized by TEM, as revealed a typical core-shell structure in which the PLGA cores were enclosed by a layer of membrane (Figure 3A). Then, protein compositions of RBC-NP-50 were analyzed by SDS-PAGE. It was shown that RBC-NP-50 shared a large similarity of protein profiles to those in RBC vesicles (Figure 3B). Furthermore, typical proteins such as CD47 and CD36 in RBC-NP-50 were characterized by Western Blot, indicating the successful transfer of cell membrane proteins. Since the natural membrane covers onto the synthetic PLGA cores, we therefore sought to investigate if RBC-NP-50 exhibit any impact on the viability of normal cells (Figure 3C). To test this, various concentrations of RBC-NP-50 (all RBC-NP-50 concentrations are expressed in terms of RBC membrane protein thereafter) were co-incubated with two

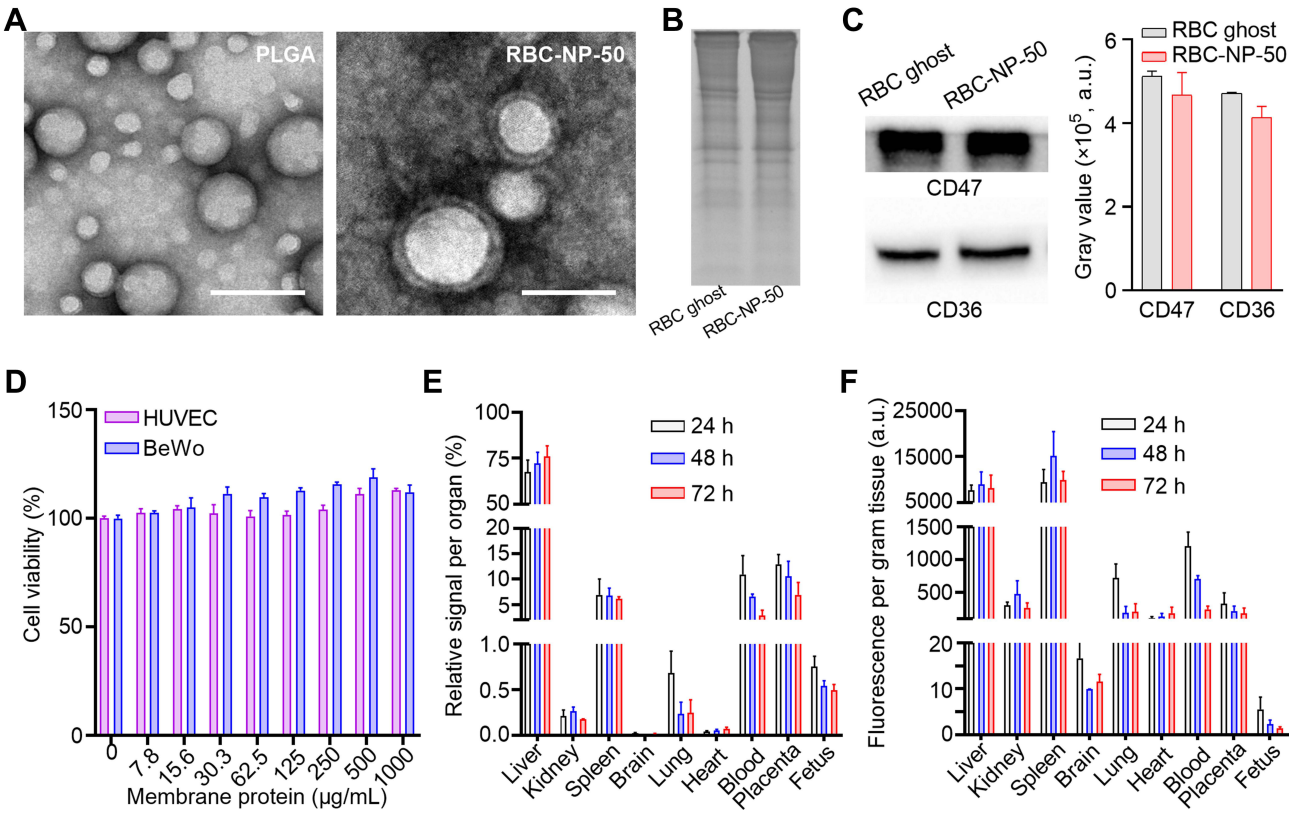

Figure 3 Characterization of RBC-NP-50. (**A**) TEM images of bare PLGA (left) and coated with RBC membrane (right). Bar = 50 μm. (**B**) SDS-PAGE protein analysis of RBC ghost and RBC-NP-50. Samples were stained with Coomassie Blue. (**C**) Typical proteins including CD47 and CD36 on RBC ghost and RBC-NP-50 with an equivalent protein were determined by Western Blot. n = 3, mean ± SD. (**D**) Cytotoxicity of RBC-NP-50 at different concentrations on HUVEC and BoWo cells. n = 3, mean ± SD. Biodistribution of the DiD-labelling RBC-NP-50 at 50 mg/kg upon intravenous injection into the pregnant mouse at GD15. At each time point (24, 48, and 72 h), the organs from mice were collected, homogenized, and quantified for fluorescent signal. Fluorescence intensity per gram of tissue (**E**) and relative signal per organ (**F**) were compared (n = 3, mean ± SD).

cell lines that are partially representative of placental structure, including a human placental choriocarcinoma cell line (BeWo) and a human umbilical vein endothelial cells (HUVEC) cell line. The results showed that RBC-NP-50 did not impact cell viability even concentration up to 1000 μg/mL (Figure 3D). Next, we aimed to investigate the biodistribution of RBC-NP-50 in pregnant mice at GD15. At the corresponding time points (24 h, 48 h, and 72 h) after intravenous injection of RBC-NP-50 at 50 mg/kg, pregnant mice were euthanized and their placentas, fetuses, blood, and major organs were harvested. When the amount of RBC-NP-50 was normalized to the organ weight, it oriented mainly in the liver, placenta, blood, spleen, and fetus (Figure 3E and 3F). Notably, the content of RBC-NP-50 in the fetus was decreased over time when they came to be normalized by weight, which was attributable to the rapid weight gaining of the developing fetus. This biodistribution fashion indicated that RBC-NP-50 posed a long circulation pattern and could readily pass through the placenta and then stay in the fetus over the study period.

Short-Term (48 h) Biocompatibility of RBC-NP-50 in Maternal Mice and Fetuses

Following the characterization and biodistribution of RBC-NP-50, we next examined the short-term biocompatibility of RBC-NP-50 in pregnant mice through two different dosing regimens. First, in a single high dose (1HD) regimen, 400 mg/kg of RBC-NP-50 was intravenously injected into pregnant mice at GD17; in a thrice successive low dose (3LD) regimen, 200 mg/kg of RBC-NP-50 was injected intravenously at GD15, 16, and 17. On 48 h after the final administration, pregnant mice in all groups were euthanized and the placentas, whole blood, serum, major organs, and fetuses were harvested. The placenta is a unique organ that provides nutrition and oxygen and plays a pivotal role in the maintenance of the developing fetus, we therefore first sought to test if the accumulation of RBC-NP-50 in placenta negatively impacted its functionality. Specifically, CYP11A1 and 3β-HSD that are involved in the steroid biosynthetic pathway in the placenta[25] were tested (Figure 4A). It was noted that mice have been treated by both 1HD and 3LD of RBC-NP-50 exhibited negligible impair against the expression of CYP11A1 and 3β-HSD in placenta, in comparison to controls. Furthermore, the serum level of progesterone, a typical steroid hormone that plays a major role in regulation of female reproduction,[26] was measured then. It was confirmed that neither 1HD nor 3LD of RBC-NP-50 had a significant effect on progesterone synthesis (Figure 4B). Additionally, little influence on angiogenesis within the placenta was also detected after two treatments (Figure 4C). Besides these, proinflammatory factors including MCP-1, TNF-α, and IL-6 in treated groups were tested and displayed all comparable to control groups (Figure 4D), and blood routine including white blood cell (WBC), platelet (PLT), and red blood cell (RBC) and biochemical assessment of important hepatic and renal parameters also showed no significant differences compared to control groups (Figure 4E and F). Likewise, histological analysis of major organs (including the heart, liver, lungs, spleen, and kidneys) and placentas revealed no noticeable irregularities (Supplementary Figure 3). These results suggested that short-term (48 h) exposure of either 1HD or 3LD of RBC-NP-50 to pregnant mice were not acutely toxic upon administration for maternal mice.

On the other hand, effective enrichment of RBC-NP-50 in fetal brain was visualized previously, providing rationale to study if the RBC-NP-50 could disrupt the development of the fetal brain. First, the 1HD and 3LD of RBC-NP-50 dosing regimens did not affect the morphology of fetuses (Figure 5A), fetal weight (Figure 5B), and the number of fetuses (Figure 5C). These results suggested that RBC-NP-50 was generally biocompatible to fetus. We then aimed to utilize high-throughput mRNA sequencing to investigate if the transcriptomic changes in the fetal brain would be induced by RBC-NP-50. The differential gene expression (DGE) analysis revealed that there were 498 and 77 genes referred to the interpretation of differences in the abundance of transcripts in fetal brains after being treated by 1HD or 3LD of RBC-NP -50, respectively, as shown in volcano maps (Figure 5D and E). Furthermore, these ranked genes could be categorized into different biological pathways through KEGG analysis. In the KEGG bubble diagram, 15 important pathways in fetal brains at 48 h after treatment with 1HD of RBC-NP-50 were identified, including inflammation, neurodevelopment, immune development, etc (Figure 5F). Noteworthily, the pathway that regarding neuroactive ligand–receptor interaction ranked as top 1 of differential gene enrichment along with the highest score of 2.49, indicating potentially acute impact on neurodevelopment initiated by 1HD of RBC-NP-50. When looking at 3LD of RBC-NP-50 treatment, moderate changes in differential gene expressions in fetal brains were detected, involving three pathways screened by KEGG analysis (Figure 5G). Overall, pregnant mice after being treated by 1HD or 3LD of RBC-NP-50 following a short term

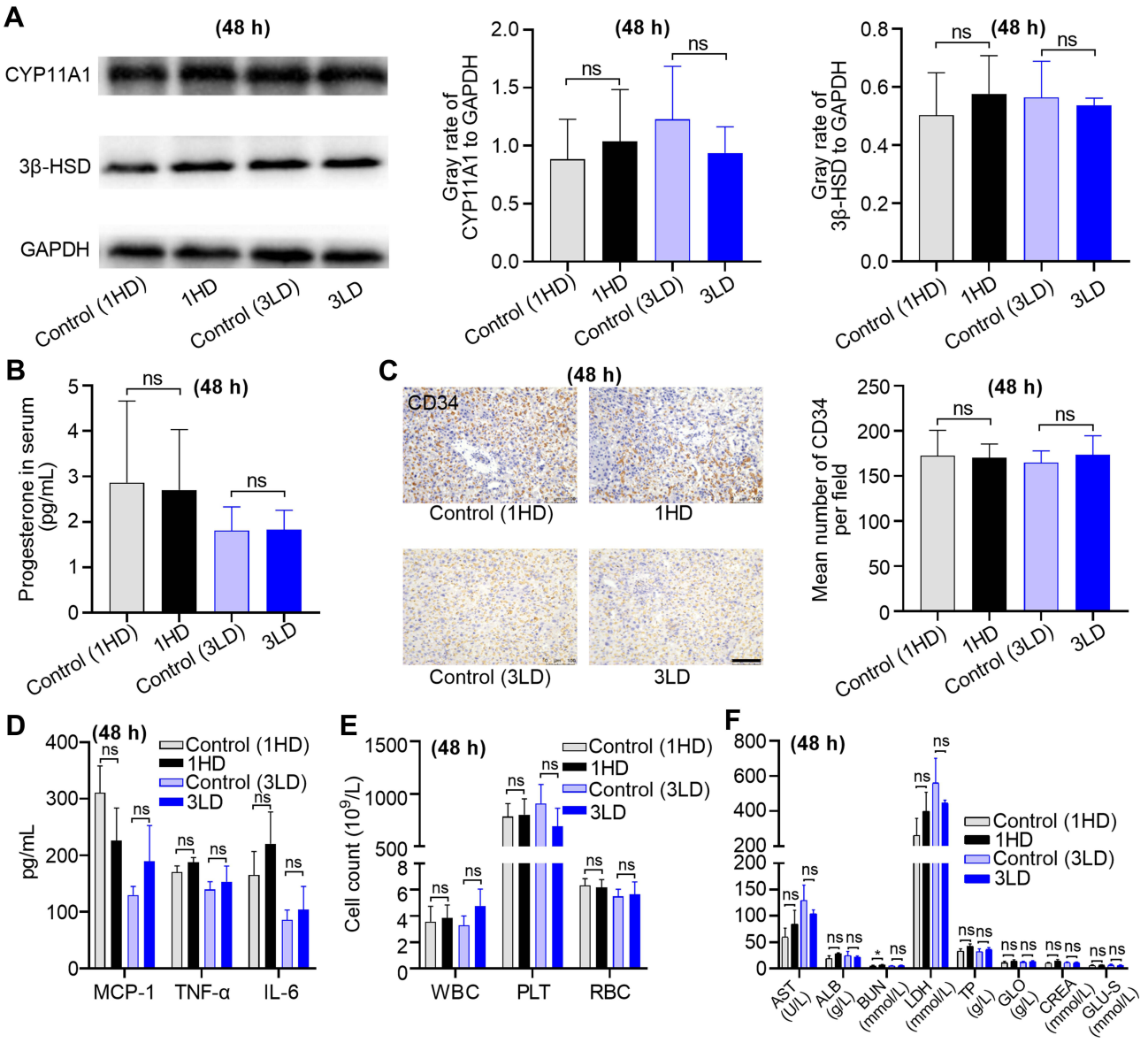

Figure 4 Short-term (48 h) biocompatibility of RBC-NP-50 to maternal mice. (**A**) CYP11A1 and 3β-HSD expressions in placenta determined by Western Blot. Statistical analysis of gray rates of tested proteins to GAPDH. n = 3, mean ± SD. (**B**) Progesterone level in blood as measured by ELISA. n = 3, mean ± SD. (**C**) Histological analysis of placenta against CD34 and photographed. Bar = 100 μm. Statistical analysis of CD34 counts in five fields per slide. n = 3, mean ± SD. (**D**) Inflammatory factors, including MCP-1, TNF-α, and IL-6 in blood were tested by ELISA. n = 3, mean ± SD. (**E**) White blood cell (WBC), platelet (PLT), and RBC count as measured (n = 3, mean ± SD). (**F**) Biochemical markers reflecting hepatic and renal function were tested (n = 3, mean ± SD). AST = aspartate aminotransferase, ALB = albumin, BUN (blood urea nitrogen), LDH = lactate dehydrogenase, TP = total protein, GLO = globulin, CREA = creatinine, and GLU-S = glucose-S. From (**A**–**F**), all samples were collected at 48 h after treatment of 1HD or 3LD of RBC-NP-50 by i.v. injections.

(48 h) did not affect maintenance of maternal pregnancy but had a significant impact on genes' expression in the fetal brain.

Long-Term (21 d) Biocompatibility of RBC-NP-50 in Maternal and Juvenile Mice

Although the remarkable changes in differential gene expression in the fetal brain at 48 h after 1HD or 3LD of RBC-NP -50 treatments, we still did not observe any of fetal developmental distortions, thus a long-term study should be examined. Following the same dosing regimens as the previous section, the subsequent maternal mice and neonatal mice were employed for various measurements over 21 d post-partum/birth. Bodyweight and water consumption of maternal mice were monitored from GD13 to 19 d post-partum every other day. It was found that neither bodyweight nor

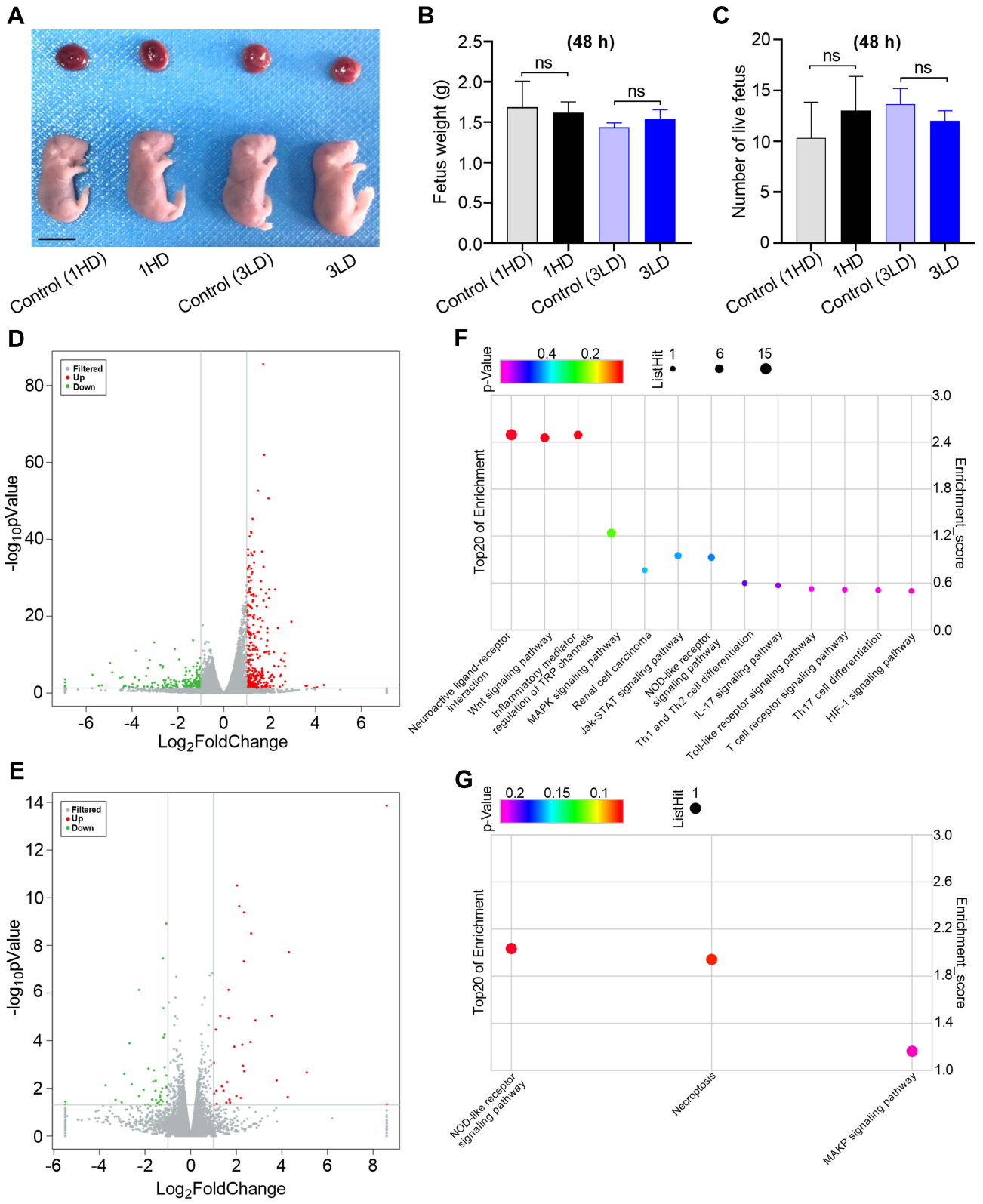

Figure 5 Short-term (48 h) biocompatibility of RBC-NP-50 to fetuses. (**A**) Images of placentas and fetuses collected from maternal mice. Scale bar = 1 cm. (**B**) Statistical analysis of fetus weight. n = 5, mean ± SD. (**C**) Statistical analysis on enumeration of live fetus per maternal mice. n = 5, mean ± SD. From (**A**–**C**), fetuses were collected at 48 h after treatment of 1HD or 3LD of RBC-NP-50 by i.v. injection. Volcano maps showing the differential gene expression in fetal brains at 48 h after being treated by 1HD (**D**) or 3LD (**E**) of RBC-NP-50 compared to controls. Gray dots express as non-significantly different genes, red and green dots represent significant difference genes. n = 3. KEGG bubble diagrams showing different biological pathways regarding the differential genes 48 h after being treated by 1HD (**F**) or 3LD (**G**) of RBC-NP-50 compared to controls. Bubble size correlates to the number of differential genes. n = 3.

https://doi.org/10.2147/IJN.S384906 DovePress

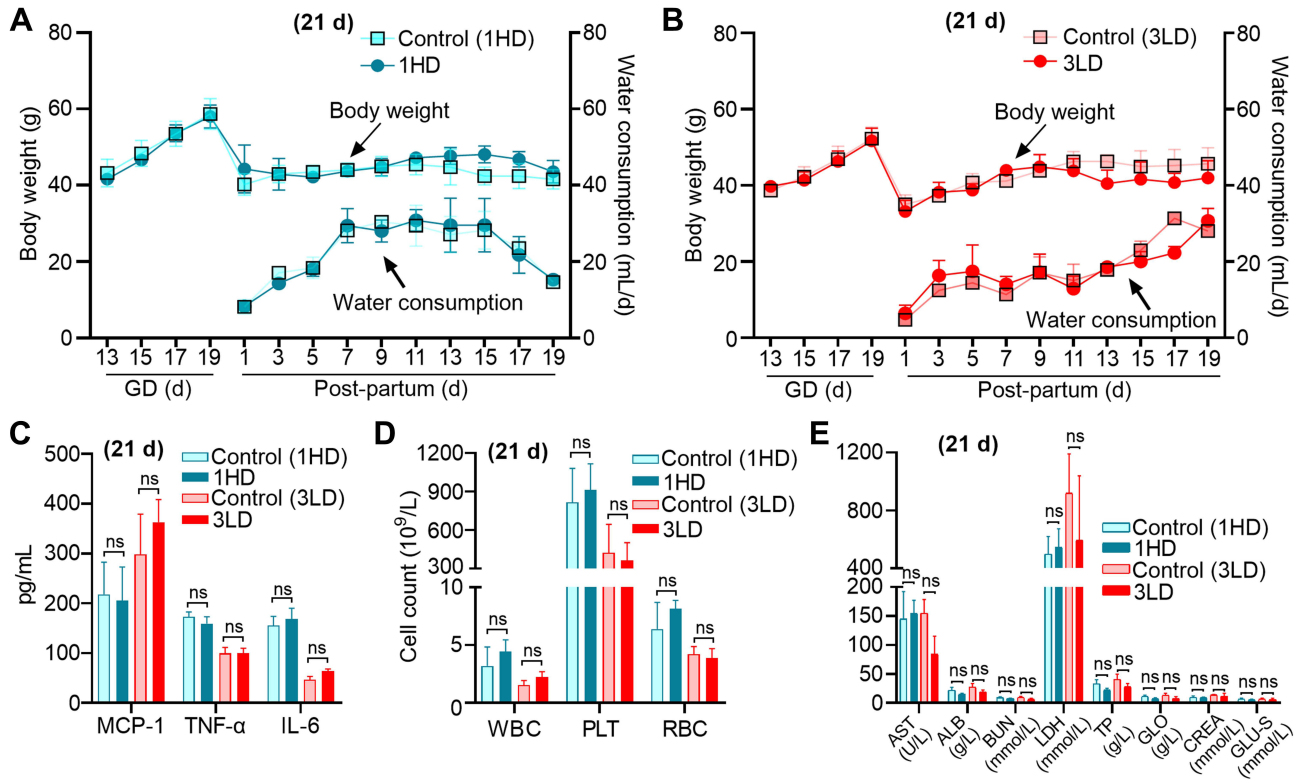

Figure 6 Long-term (21 d) biocompatibility of RBC-NP-50 to maternal mice. Body weight gaining and water consumption of maternal mice as monitored from GD13 to 21 d post-partum, in both 1HD (**A**) or 3LD (**B**) groups. n = 5, mean ± SD. (**C**) Inflammatory factors, including MCP-1, TNF-α, and IL-6 in blood were tested by ELISA. n = 3, mean ± SD. (**D**) WBC, PLT, and RBC count as measured (n = 3, mean ± SD). (**E**) Biochemical markers reflecting hepatic and renal function were tested, including AST, ALB, BUN, LDH, TP, GLO, CREA, and GLU-S. (n = 3, mean ± SD). From (**C–E**), all parameters were measured upon maternal mice at 21 d post-partum.

water consumption showed significant differences in 1HD or 3LD groups when compared to the respective controls (Figure 6A and B). Also, the representative proinflammatory factors (Figure 6C), major hematology-related markers (Figure 6D), and clinical biochemical assessment for hepatic and renal functions (Figure 6E) showed no significant differences between treatments and controls. These results were consistent with those tested in short-term evaluation, confirming the great biocompatibility of RBC-NP-50 to maternal mice.

When paying attention on their offspring, it is just known that exposure of RBC-NP-50 to fetus was capable of causing the considerable changes on different genes' expression in the fetal brain; thus, we sought to investigate that if these differences would affect the development of neonatal/juvenile mice. First, the number of live newborn in groups treatment with 1HD or 3LD of RBC-NP-50 was all comparable to the respective controls (Figure 7A). Afterwards, the weight gaining curves of juvenile mice exhibited no significantly different among all groups (Figure 7B). In addition, typical behavioral assessments were done upon juvenile mice, including surface righting, negative geotaxis, cliff avoidance, and olfactory orientation tests (Figure 7C). Juvenile mice in all groups were evaluated for behaviors on a 0–2 scale based on different abnormal activities for each behavioral experiment. We found that there were no significant differences in scoring various behaviors in all groups. Likewise, when analyzing the transcriptome of brains from juvenile mice at 21 d post-birth, only 15 and 28 genes showed significantly changed after treatment with 1HD and 3LD of RBC-NP-50, respectively (Figure 7D and E), in comparison with many more changes in short-term treatments (48 h). This result was noted that the acute impact on the fetal brain after RBC-NP -50 exposure seems like a temporal phenomenon, and it might be alleviated over time during brain development after birth. Furthermore, the obtained different genes' expression between two treatment groups could be also summarized into inflammatory related genes using KEGG analysis (Figure 7F and G). When together with previous results of short-term exposure of RBC-NP-50 to the fetus, we found that the inflammatory process was most likely a common

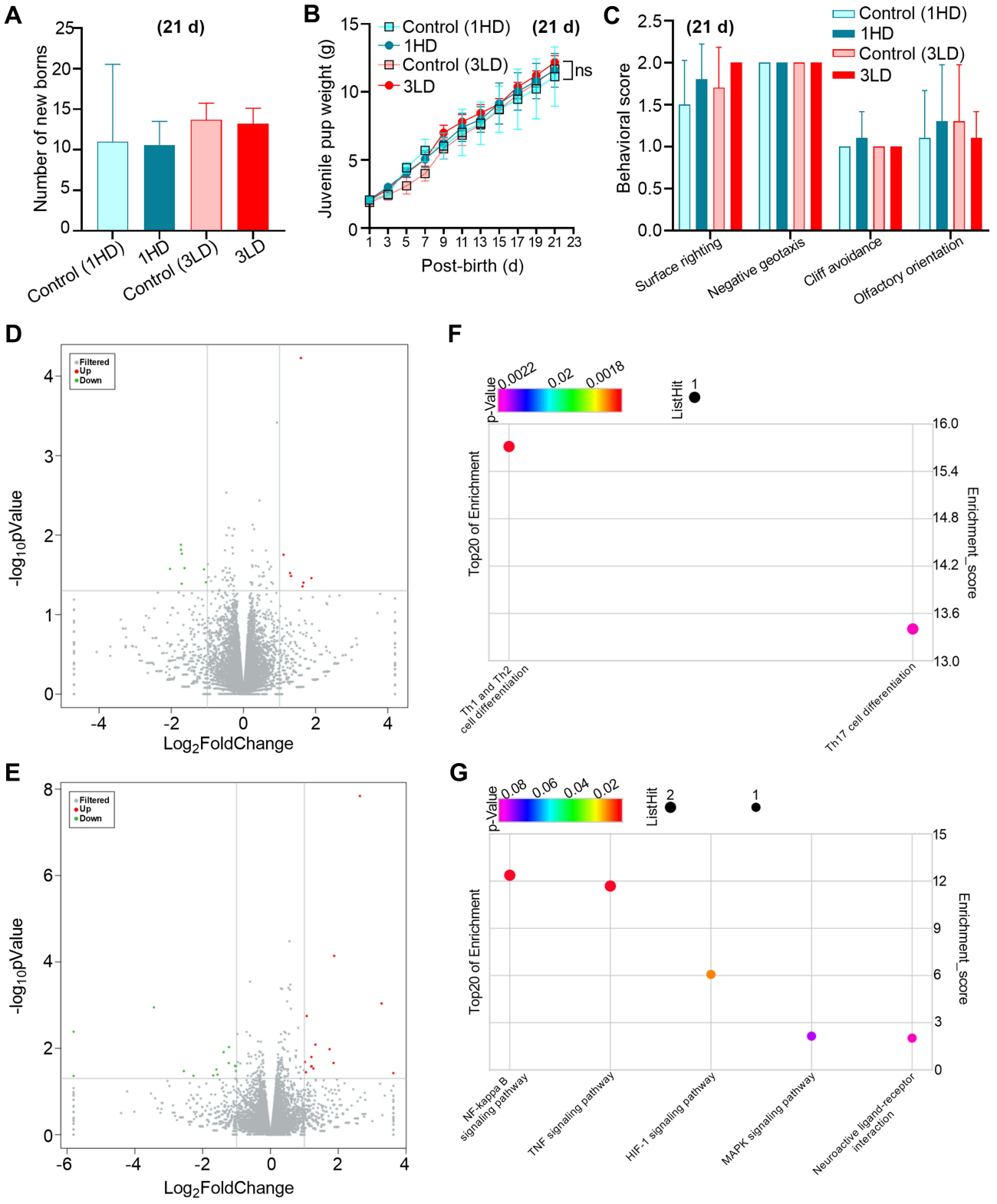

Figure 7 Long-term (21 d) biocompatibility of RBC-NP-50 to juvenile mice. (**A**) Statistical analysis on enumeration of newborns per maternal mice. n = 5, mean ± SD. (**B**) Body weight gaining of juvenile mice. n = 5, mean ± SD. (**C**) Behavioral evaluations on juvenile mice, including surface righting, negative geotaxis, cliff avoidance, and olfactory orientation tests. n = 10, mean ± SD. From (**A**–**C**), the related measurements were performed from 1 d to 21 d post-birth after treatment of 1HD or 3LD of RBC-NP-50 by i.v. injections. Volcano maps showing the differential gene expression in juvenile brains at 21 d post-birth treated by 1HD (**D**) or 3LD (**E**) of RBC-NP-50 compared to controls. Gray dots express non-significantly different genes, red and green dots represent significant difference genes. n = 3. KEGG bubble diagrams showing different biological pathways regarding the differential genes at 21 d post-birth after being treated by 1HD (**F**) or 3LD (**G**) of RBC-NP-50 compared to controls. Bubble size correlates to the number of differential genes. n = 3.

https://doi.org/10.2147/IJN.S384906 DovePress

pathway that was responsible for RBC-NP-50's influence. In addition to KEGG bubble diagram, the specific genes for each enriched bubble have been listed in the heatmap fashion, as shown in Supplementary Figure 4.

Conclusion

In this study, we have developed an ultra-small RBC membrane-based biomimetic nanoparticle (RBC-NP-50) at an average size of nearly 50 nm. With the merit of small size, RBC-NP-50 were capable of crossing through the BFB efficiently and orienting into the fetus, thereby providing an opportunity to investigate the dose-dependent toxicity of RBC-NP in both maternal and fetal/juvenile mice. After dosing with 1HD or 3LD of RBC-NP-50, all measured parameters showed little change in maternal mice neither after 48 h during pregnancy nor 21 d post-partum. When looking at fetus, 1HD of RBC-NP-50 exposure strongly impacted genes' expression that was mainly responsible for inflammation, neurodevelopment, immune development, etc, whereas 3LD dosing regimen exhibited mild influences. Nonetheless, those altered expressed genes in the fetal brain would be gradually restored as mice developing post-birth, as corroborated by negligible behavioral differences and decreased number of differential expressed genes in juvenile mice on 21 d post-birth. Overall, the RBC-NP is generally biosafe to maternal mice and their offspring, but we still need to note that the toxicity of RBC-NP itself should not be overlooked when it comes to high dosage.

Abbreviations

PLGA, poly(lactic-*co*-glycolic) acid; RBC, red blood cell; RBC-NP, PLGA nanoparticle coated with RBC membrane; RBC-NP-50, RBC-NP with 50 nm in diameter; RBC-NP-180, RBC-NP with 180 nm in diameter; RBC-NP-400, RBC-NP with 400 nm in diameter; RBC-NP-1000, RBC-NP with 1000 nm in diameter; 1HD, a single high dose of RBC-NP -50 at 400 mg/kg; 3LD, an thrice successive low dose of RBC-NP-50 at 200 mg/kg; GD, gestation day; BFB, blood–fetal barrier; BBB, blood-brain barrier; RT, room temperature; DLS, dynamic laser scattering; TEM, transmission electron microscopy; CYP11A1, cytochrome P450 family 11 subfamily A member 1; 3β-HSD, 3β-hydroxysteroid dehydrogenase; IL-6, interleukin 6; TNF-α, tumor necrosis factor α; MCP-1, monocyte chemoattractant protein-1; GO, Gene Ontology; KEGG, Kyoto Encyclopedia of Genes and Genomes; DEGs, differentially expressed genes.

Acknowledgments

This work is supported by the Outstanding Youth Fund Project of Zhejiang Natural Science Foundation No. LR22H150001 (Y.C.), Key Projects Jointly Constructed by Zhejiang Province and the Ministry No. WKJ-ZJ-2339 (Y. C.), Major Innovation Project of Wenzhou Science and Technology Bureau No. 2021ZY0002 (Y.C.), Natural Science Foundation of China No. 81701828 (Y.C.), No. 82071626 (P.D.). We would like to thank Shanghai OE Biotechnology Co., Ltd. for analyzing RNA-seq. Also, we would like to thank the Scientific Research Center of Wenzhou Medical University for consultation and instrument availability and WenZhou DaTong Biotech Co., Ltd (Wenzhou, China) that supported this work.

Disclosure

The authors report no conflicts of interest in this work.

References

1. Fang RH, Hu C-MJ, Zhang L. Nanoparticles disguised as red blood cells to evade the immune system. *Expert Opin Biol Ther*. 2012;12:385–389. doi:10.1517/14712598.2012.661710
2. Hu C-MJ, Zhang L, Aryal S, et al. Erythrocyte membrane-camouflaged polymeric nanoparticles as a biomimetic delivery platform. *Proc Natl Acad Sci USA*. 2011;108:10980–10985. doi:10.1073/pnas.1106634108
3. Malhotra S, Dumoga S, Singh N. Red blood cells membrane-derived nanoparticles: applications and key challenges in their clinical translation. *Wiley Interdiscip Rev Nanomed Nanobiotechnol*. 2022;14:e1776. doi:10.1002/wnan.1776
4. Nemati E. gholami, ahmad. Cell membrane coated nanoparticles for biomedical applications. *Adv Appl Nanobio-Technologies*. 2022;3:49–59.
5. Gao W, Zhang L. Engineering red-blood-cell-membrane–coated nanoparticles for broad biomedical applications. *AiChE J*. 2015;61:738–746. doi:10.1002/aic.14735
6. Xia Q, Zhang Y, Li Z, Hou X, Feng N. Red blood cell membrane-camouflaged nanoparticles: a novel drug delivery system for antitumor application. *Acta Pharm Sin B*. 2019;9:675–689. doi:10.1016/j.apsb.2019.01.011

7. Copp JA, Fang RH, Luk BT, et al. Clearance of pathological antibodies using biomimetic nanoparticles. *Proc Natl Acad Sci U S A*. 2014;111:13481–13486. doi:10.1073/pnas.1412420111
8. Chen Y, Chen M, Zhang Y, et al. Broad-spectrum neutralization of pore-forming toxins with human erythrocyte membrane-coated nanosponges. *Adv Healthc Mater*. 2018;7(1701366):1701366
9. Hu CMJ, Fang RH, Copp J, et al. A biomimetic nanosponge that absorbs pore-forming toxins. *Nat Nanotechnol*. 2013;8:336–340. doi:10.1038/nnano.2013.54
10. Escajadillo T, Olson J, Luk BT, Zhang L, Nizet V. A red blood cell membrane-camouflaged nanoparticle counteracts Streptolysin O-mediated virulence phenotypes of invasive Group A Streptococcus. *Front Pharmacol*. 2017;8(477). doi:10.3389/fphar.2017.00477
11. Pang Z, Hu C-MJ, Fang RH, et al. Detoxification of organophosphate poisoning using nanoparticle bioscavengers. *ACS Nano*. 2015;9:6450–6458. doi:10.1021/acsnano.5b02132
12. Hu C-MJ, Fang RH, Luk BT, Zhang L. Nanoparticle-detained toxins for safe and effective vaccination. *Nat Nanotechnol*. 2013;8:933–938. doi:10.1038/nnano.2013.254
13. Wei X, Gao J, Wang F, et al. In situ capture of bacterial toxins for antivirulence vaccination. *Adv Mater*. 2017;29(1701644):1701644. doi:10.1002/adma.201701644
14. Luk BT, Fang RH, Hu C-MJ, et al. Safe and immunocompatible nanocarriers cloaked in RBC membranes for drug delivery to treat solid tumors. *Theranostics*. 2016;6:1004–1011. doi:10.7150/thno.14471
15. Su J, Liu G, Lian Y, et al. Preparation and characterization of erythrocyte membrane cloaked PLGA/arsenic trioxide nanoparticles and evaluation of their in vitro anti-tumor effect. *RSC Adv*. 2018;8:20068–20076. doi:10.1039/C8RA01417E
16. Fang RH, Hu C-MJ, Chen KNH, et al. Lipid-insertion enables targeting functionalization of erythrocyte membrane-cloaked nanoparticles. *Nanoscale*. 2013;5:8884–8888. doi:10.1039/c3nr03064d
17. Bidkar AP, Sanpui P, Ghosh SS. Transferrin-conjugated red blood cell membrane-coated poly(lactic-co-glycolic acid) nanoparticles for the delivery of doxorubicin and methylene blue. *ACS Appl Nano Mater*. 2020;3:3807–3819. doi:10.1021/acsanm.0c00502
18. Wu X, Li Y, Raza F, et al. Red blood cell membrane-camouflaged tedizolid phosphate-loaded PLGA nanoparticles for bacterial-infection therapy. *Pharmaceutics*. 2021;13(99):99. doi:10.3390/pharmaceutics13010099
19. Bongaerts E, Nawrot TS, Van Pee T, Ameloot M, Bové H. Translocation of (ultra)fine particles and nanoparticles across the placenta; a systematic review on the evidence of in vitro, ex vivo, and in vivo studies. *Part Fibre Toxicol*. 2020;17:56. doi:10.1186/s12989-020-00386-8
20. Liao Y, Zhang Y, Blum NT, Lin J, Huang P. Biomimetic hybrid membrane-based nanoplatforms: synthesis, properties and biomedical applications. *Nanoscale Horizons*. 2020;5:1293–1302. doi:10.1039/D0NH00267D
21. Dehaini D, Wei X, Fang RH, et al. Erythrocyte-platelet hybrid membrane coating for enhanced nanoparticle functionalization. *Adv Mater*. 2017;29:1606209. doi:10.1002/adma.201606209
22. Gao M, Liang C, Song X, et al. Erythrocyte-membrane-enveloped perfluorocarbon as nanoscale artificial red blood cells to relieve tumor hypoxia and enhance cancer radiotherapy. *Adv Mater*. 2017;29:35. doi:10.1002/adma.201701429
23. Yan J, Yu J, Wang C, Gu Z. Red blood cells for drug delivery. *Small Methods*. 2017;1:1700270. doi:10.1002/smtd.201700270
24. Fan Z, Li PY, Deng J, Bady SC, Cheng H. Cell membrane coating for reducing nanoparticle-induced inflammatory responses to scaffold constructs. *Nano Res*. 2018;11:5573–5583. doi:10.1007/s12274-018-2084-y
25. Zhu H-L, Shi X-T, Xu X-F, et al. Environmental cadmium exposure induces fetal growth restriction via triggering PERK-regulated mitophagy in placental trophoblasts. *Environ Int*. 2021;147:106319. doi:10.1016/j.envint.2020.106319
26. Tuckey RC. Progesterone synthesis by the human placenta. *Placenta*. 2005;26:273–281. doi:10.1016/j.placenta.2004.06.012
27. Luk BT, Jack Hu C-M, Fang RH, et al. Interfacial interactions between natural RBC membranes and synthetic polymeric nanoparticles. *Nanoscale*. 2014;6:2730–2737. doi:10.1039/C3NR06371B